Exploration of Key Regulatory Factors in Mesenchymal Stem Cell Continuous Osteogenic Differentiation via Transcriptomic Analysis

Yu Pan , Tao Liu , Linfeng Li , Liang He , Shu Pan * , Yuwei Liu *

Posted Date: 18 October 2024

doi: 10.20944/preprints202410.1444.v1

Keywords: MSCs; lineage change; transcriptomic sequencing; dynamic regulation; osteogenesis

 doi:10.20944/preprints202410.1444.v1

Article

Exploration of Key Regulatory Factors in Mesenchymal Stem Cell Continuous Osteogenic Differentiation via Transcriptomic Analysis

Yu Pan [1,2], Tao Liu [1,2], Linfeng Li [3], Liang He [4], Shu Pan [5,*] and Yuwei Liu [1,*]

[1] Department of Bioinformatics and Intelligent Diagnosis, School of Medicine, Jiangsu University, 212013 Zhenjiang, China
[2] Department of Orthopaedic Surgery, Zhenjiang First People's Hospital,212002 Zhenjiang, China
[3] Department of Orthopaedics, 958 Hospital of PLA Army, 400020 Chongqing, China
[4] Tongji University School of Medicine, 201619 Shanghai, China
[5] Computer Science School, Jiangsu University of Science and Technology, 212003 Zhenjiang, China
* Correspondence: liuyuwei@ujs.edu.cn; jsjxy_ps@just.edu.cn

Abstract: Background/Objectives: Mesenchymal Stem Cells (MSCs) possess the remarkable ability to differentiate into various cell types, including osteoblasts. Understanding the molecular mechanisms governing MSC osteogenic differentiation is crucial for advancing clinical applications and our comprehension of complex disease processes. However, the key biological molecules regulating this process remain incompletely understood, necessitating further investigation. **Methods**: In this study, we employed high-throughput transcriptomic sequencing to identify and validate key biological molecules that dynamically regulate MSC osteogenic differentiation. Our approach involved comprehensive analysis of gene expression patterns across human tissues, followed by rigorous experimental validation of identified candidates. **Results**: Through our integrated analytical and experimental approach, we pinpointed four critical regulators of MSC osteogenic differentiation: PTBP1, H2AFZ, BCL6, and TTPAL (C20ORF121). Notably, this study represents the first instance of utilizing high-throughput transcriptomics to uncover regulatory factors involved in MSC osteogenesis, marking a significant advancement in the field. **Conclusions**: Our findings substantially enhance our understanding of the molecular mechanisms determining MSC differentiation fate. This research holds significant implications for clinical applications involving MSCs and provides valuable insights into complex disease processes. The identification of these key regulators opens new avenues for targeted interventions and therapies in bone-related disorders and regenerative medicine. Furthermore, this study establishes a robust framework for future investigations in stem cell biology, potentially leading to innovative approaches in regenerative medicine.

Keywords: MSCs; lineage change; transcriptomic sequencing; dynamic regulation; osteogenesis

1. Introduction

Mesenchymal stem cells (MSCs) possess the ability to differentiate into diverse cell lineages [1,2], rendering them indispensable for maintaining physiological homeostasis, as well as promoting tissue regeneration and repair [3,4]. MSCs are ubiquitously distributed across multiple tissues and constitute a multipotent progenitor cell population with clonogenic potential [5,6]. Consequently, MSCs have garnered significant attention owing to their immense therapeutic potential in regenerative medicine [7,8]. The fate determination of MSCs is tightly regulated by intricate interactions among numerous cell factors derived from the tissue microenvironment [9], which act as molecular switches for lineage differentiation through specific activation or dysfunction mechanisms [10]. Understanding the molecular mechanisms that determine the MSC fate is essential for

 doi:10.20944/preprints202410.1444.v1

implementing targeted strategies to correct abnormal lineage distribution, particularly in conditions such as osteoporosis and bone aging [11,12].

Previous studies have identified several cellular factors, such as Runx2 [13,14] and Osterix [15,16], as key regulators of MSC differentiation, particularly in promoting osteogenic lineage differentiation [17,18]. Genomics has furthered research conducted in the field of genome-wide dynamics of transcription factor binding and epigenome programming during preosteoblast differentiation [19,20]. However, further research is required to elucidate the dynamics of chromosome structure and enhancer activity during osteogenesis in MSC lineage studies [21,22]. To date, no studies have systematically explored the cellular factors that continuously regulate MSC differentiation into the osteogenic lineage across different time points, hindering comprehensive evaluation of osteoporosis [23,24]. Therefore, it is crucial to conduct systematic investigations into the cellular factors governing MSC lineage fate to identify key elements that influence MSC differentiation [25,26].

In this study, we performed a systematic analysis of differentially expressed genes (DEGs) by integrating high-throughput sequencing data related to human MSC differentiation into the osteogenic lineage. Subsequently, we identified DEGs with significant differential expression across multiple time points and validated the candidate genes exhibiting high expression in bone marrow tissue under screening conditions by comparing them to 45 human tissues from the HUMAN PROTEIN ATLAS database. Finally, we performed biological experiments to verify the ability of the selected candidates to continuously regulate the osteogenic induction of MSCs. Our study established a foundational framework for identifying candidates with enhanced clinical relevance for the treatment of osteoporosis and bone fracture healing.

2. Materials and Methods

Cell culture

Primary mBMSCs were isolated from the femur bone marrow of 2-month-old wild-type C57BL/6J mice. The isolated cells were stored in BMSC medium (DMEM medium containing 20% heat-inactivated FBS) for 1 day. On the second day, the supernatant (including osteoclasts) was removed, and the adherent hematopoietic cells were removed by intensive washing with phosphate-buffered saline (PBS) for three times. The culture was continued with a fresh BMSC medium. After 2 weeks, the growth colonies were collected by trypsinization for further passage and differentiation.

Cell differentiation

BMSCs were cultured in alpha-modified Eagle's minimum essential medium supplemented with 10% FBS, 200 mM L-glutamine (25030081, Gibco) and nonessential amino acids (NEAA, 11140050, Gibco).

Osteogenic differentiation: 100 mM ascorbic acid, 2 mM b-glycerophosphate, and 10 nM dexamethasone (D4902; Sigma–Aldrich, USA).

For adipogenic differentiation, 0.5 mM isobutylmethylxanthine (IBMX, HY-12318, MCE), 0.5 mM hydrocortisone (803146, Sigma–Aldrich, USA), and 60 mM indomethacin (I7378, Sigma–Aldrich, USA) were used.

Media were changed every 2 days.

Lentivirus transduction

Lentiviral transduction: Lentiviruses overexpressing genes were purchased from Genomeditech.

BMSCs were infected with the virus. After 48 h transfection, the cells underwent osteogenic-induced differentiation.

Quantitative real-time PCR

Total RNA was extracted and isolated using total RNA extraction reagent (TRIzol, Sangon, B511311-0025). Reverse transcription was performed using HiScript II Q RT SuperMix (Vazyme, R222-01). Real-time quantitative fluorescent PCR (qPCR) was conducted using a real-time PCR system (Thermo Fisher) with Hieff SYBR Green Master Mix (Low RoxPlus) for real-time quantitative fluorescent PCR (Yeasen, 11202ES03). The experiment was repeated three times. The values were normalized to those of GAPDH. The sequences of the primers used are listed in Table S1.

 doi:10.20944/preprints202410.1444.v1

Alizarin red staining (ARS)

The cell-abandoned medium was immersed in alizarin red S staining solution for 30 min. The cells were quickly rinsed with distilled water and then studied under a microscope.

Alcian blue staining

The cells were washed with PBS for three times for 3 min each and then fixed with 4% paraformaldehyde. Next, cells were washed with PBS again and incubated with 1% of alcian blue for 30 min. Then cells were rinsed in water for 2 min and dehydrated with 95% ethanol for 15 sec. Ultimately, the slides were observed under a microscope.

Oil red O staining

The cells were immobilized with phosphate buffer containing 10% formaldehyde for 10 min and then rinsed once with PBS for 1 min. Next, the cells were rinsed with 60% isopropyl alcohol for 15 s to promote neutral fat staining. Then, the cells were stained with filtered oil red O working solution at 37°C for 30 min, treated with 60% isopropyl alcohol for 30 s, and rinsed with PBS for three times for 3 min each. Finally, the cells were observed under a microscope.

ALP staining

After 7 days of osteogenic induction, the cells were washed with PBS for three times and then fixed with 4% paraformaldehyde. Subsequently, the cells were incubated with a solution containing 5-bromo-4-chloro-3-indolyl phosphate/nitro blue tetrazolium. After 15 min of incubation at 37°C, the cell layer was washed with deionized water for three times and observed under a digital camera.

3. Results

3.1. Subsection

1. **Integration analysis of microarray datasets to identify differentially expressed genes in MSC osteogenic differentiation**

To identify genes associated with MSC osteogenic differentiation, we performed an integration analysis on two microarray datasets with comparable levels of osteogenic induction. Specifically, the datasets utilized for our analysis were GSE37558 for 12-day osteogenic induction and GSE28205 for 14-day induction. Despite the difference in induction duration, both datasets were considered to have comparable levels of osteogenic activity, making them suitable for a combined analysis.

We employed a relaxed screening threshold with a false discovery rate (FDR) ≤ 0.25 and a P value ≤ 0.05 to detect DEGs within each dataset. Moreover, a Venn diagram analysis was used to recognize the common DEGs between the two datasets, revealing a total of 1156 shared genes (Figure 1A and 1B).

 doi:10.20944/preprints202410.1444.v1

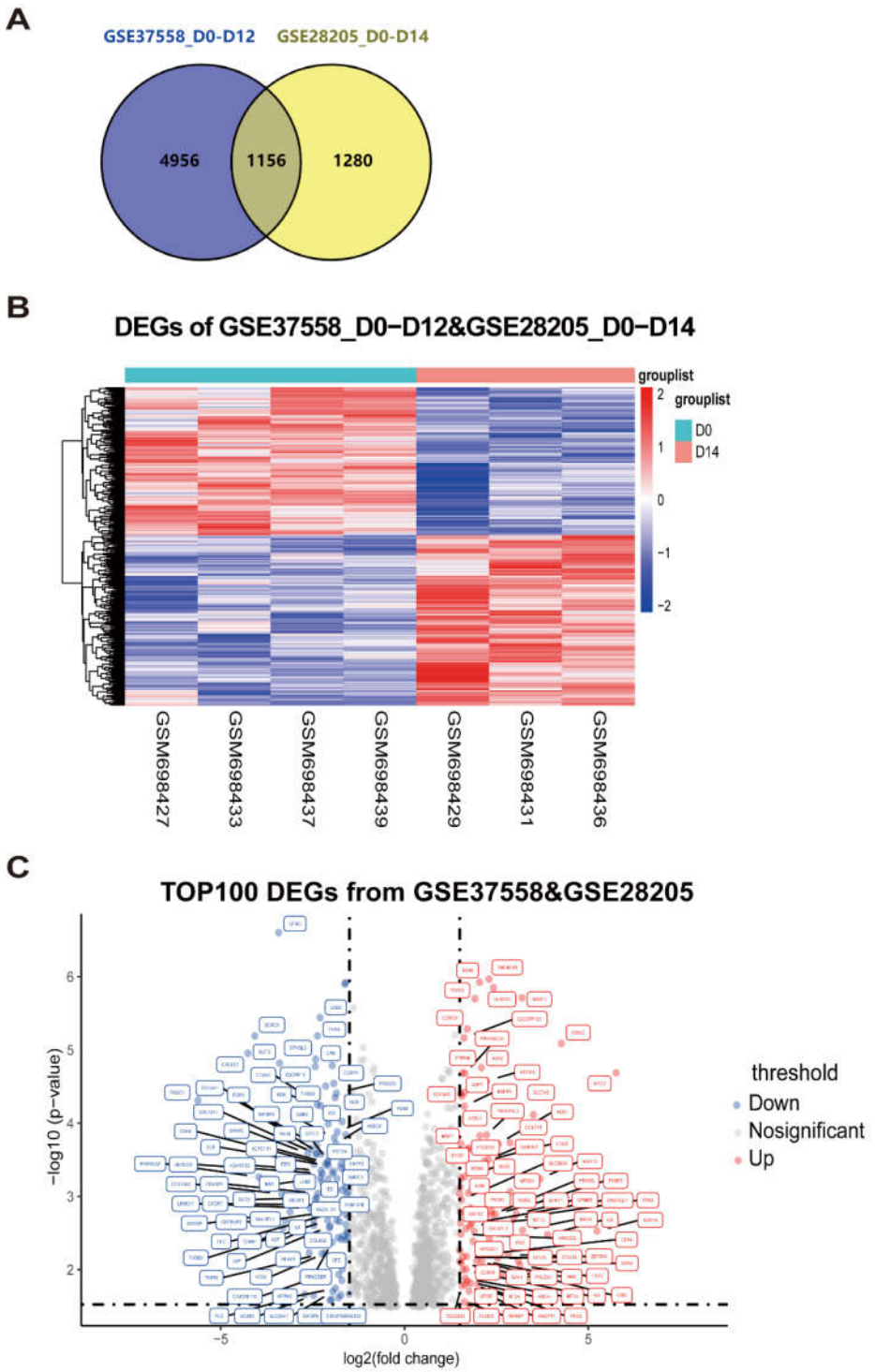

Figure 1. Two batches of microarray datasets related to long-term osteogenic induction were analyzed to identify DEGs. (A) A Venn diagram was generated to illustrate the intersection of DEGs between the two batches of microarray datasets, which were screened based on criteria with a false discovery rate (FDR) <=0.25 and a P value<=0.05. (B) A heatmap was utilized to visualize the DEGs between the two batches of datasets. (C) The volcano plot in panel B presents the information on DEGs with a cutoff value of log2(fold change)>=1.5.

To further refine the selection, we applied a cutoff of log2(fold change) ≥ 1.5, which identified 169 DEGs. Among these, 100 were down-regulated, and 69 were up-regulated, as depicted in Figure 1C. The above genes would be subjected to further experimental validation and analysis for deeper understanding of their roles in MSC osteogenic differentiation.

Preprints.org (www.preprints.org) | NOT PEER-REVIEWED | Posted: 18 October 2024 doi:10.20944/preprints202410.1444.v1

2. Exploration of continuously differentially expressed genes during MSC osteogenic induction from GSE37558 dataset

To ensure a comprehensive analysis of transcriptome dynamics during osteogenic differentiation, we integrated microarray data from GSE37558 dataset over a time course. The dataset enabled us to examine changes in gene expression across multiple time points during the differentiation process.

For our analysis, we performed time point of osteogenic induction as a reference for subsequent induction time points and analyzed the GSE37558 dataset. Specifically, we compared gene expression changes between Day 0 to 2, Day 2 to 8, and Day 8 to 25. To identify DEGs across these intervals, we applied screening criteria with a false discovery rate (FDR) of ≤ 0.25 and a P value of ≤ 0.05. This approach allowed us to detect 549 DEGs over the course of osteogenic induction, as shown in Figure 2A and 2B.

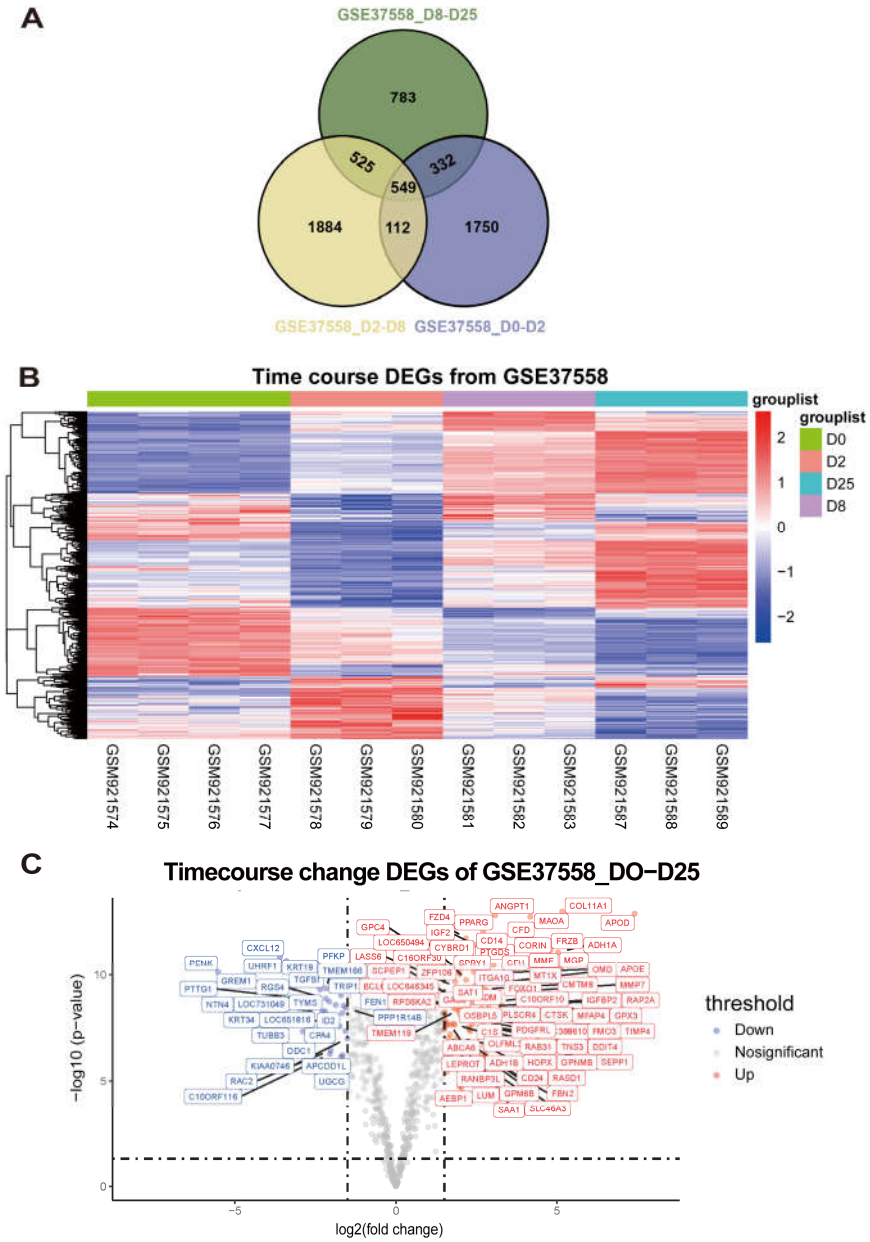

Figure 2. Refinement of time-dependent osteogenic induction in MSCs through the analysis of microarray dataset GSE37558. (A) A Venn diagram was generated to display the overlap of DEGs across three time points during osteogenic induction in the GSE37558 dataset, with screening criteria set at FDR<=0.25 and P value<=0.05. (B) The DEGs among the three different osteogenic induction

 doi:10.20944/preprints202410.1444.v1

time points in the GSE37558 dataset were visualized using a heatmap. (C) The volcano plot in panel B presents the information on DEGs with a cutoff value of log2(fold change)>=1.5.

Delving into our findings, we used a log2(fold change) threshold of ≥ 1.5, identifying 121 DEGs. Of these, 84 were up-regulated, and 27 were down-regulated (Figure 2C). These genes would undergo additional scientific investigation to further explore their roles in MSC osteogenic differentiation.

3. **Integrated time-course analysis of differentially expressed genes during MSC osteogenic induction**

We conducted an integrated time-course analysis of DEGs both with a single batch of microarray data and across multiple batches from different research groups. The approach optimized the identification of continuously differentially expressed genes during MSC osteogenic induction.

After correcting for batch effects and improving data accuracy, we combined the results from two microarray batches conducted by different research groups. The integration led to the identification of 124 genes that showed differential expression across both datasets. The relevant data are shown in Figure 3A.

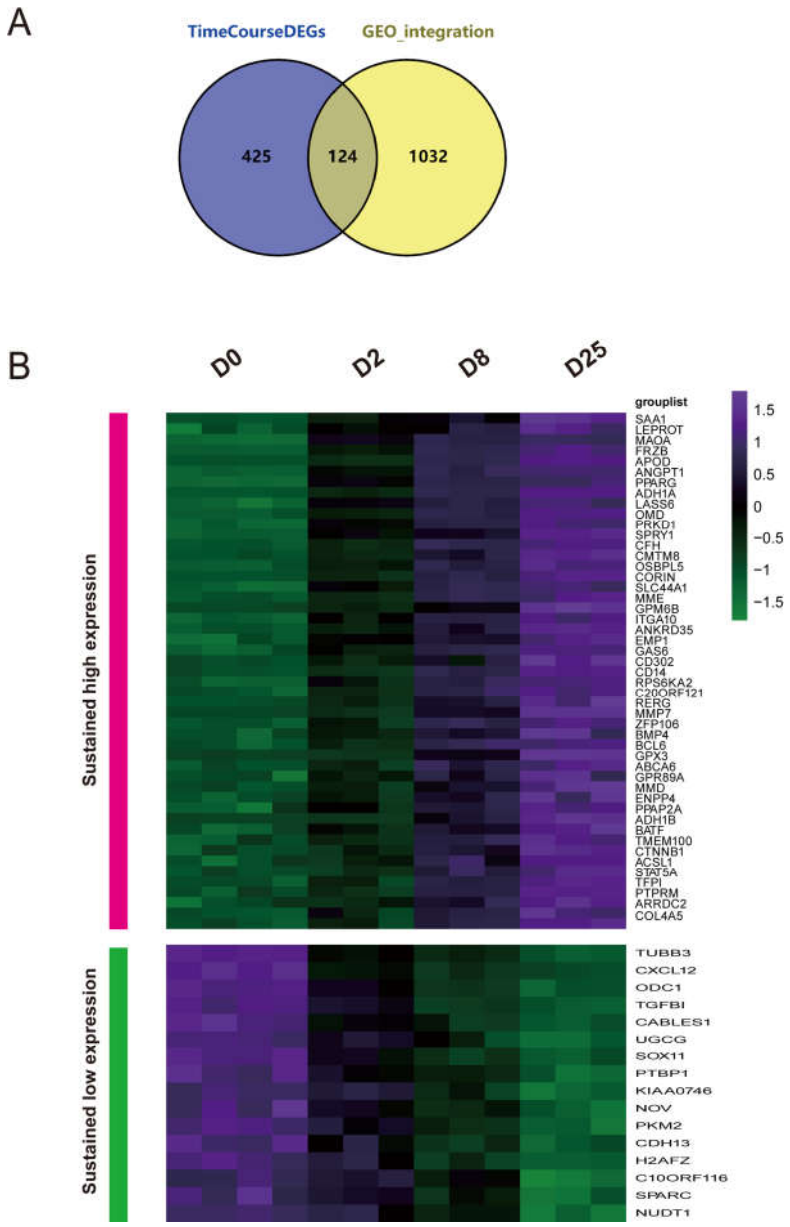

 doi:10.20944/preprints202410.1444.v1

Figure 3. Recombining DEGs to enhance the screening and identification of key regulatory molecules. (A) Venn diagram showing the intersection of DEGs across time points and microarray datasets from various batches; (B) Heatmap visualizing detailed information on the intersection of DEGs in panel A.

We subsequently applied a log2(fold change) (LOGFC) threshold of ≥ 1.5 to identify 65 genes, of which 49 genes exhibited significantly up-regulation throughout the osteogenic induction process and 16 genes showed significantly down-regulation. The corresponding data are presented in Figure 3B.

The results mentioned above suggest that the 49 up-regulated genes may play a crucial role in regulating the dynamics of MSC osteogenic differentiation. Follow-up investigations are currently underway to validate these candidate genes and explore their biological functions in the osteogenic process.

4. **Identification of key regulators governing MSC osteogenic differentiation through the HUMAN PROTEIN ATLAS database**

We focused on identifying key regulators that influence the dynamic progression of MSC osteogenic differentiation. To achieve this, we integrated the expression levels of candidate genes in human tissues using the HUMAN PROTEIN ATLAS database, which provides comprehensive data on RNA and protein expression across 45 human tissue types.

The candidate genes, previously identified as potential regulators of MSC osteogenic differentiation, were analyzed for their expression in human tissues. We leveraged the HUMAN PROTEIN ATLAS database to assess their expression levels in both RNA and protein forms, allowing us to determine the relevance of these genes in various tissues.

Previous studies have highlighted the pivotal role of bone cells, including mesenchymal stem cells and hematopoietic stem cells, in regulating cellular behavior and maintaining tissue homeostasis within the stem cell lineage [27,28]. The skeletal system contains intricate cell lineages derived from these stem cells, which dictate their differentiation into osteogenic lineage, coupled with maintaining the homeostasis of both skeletal and marrow tissues [29].

Given the importance of hematopoietic tissues in blood and immune system regulation, we examined the expression of the candidate genes in these specific tissues using data from the HUMAN PROTEIN ATLAS. A total of 13 potential key regulators were identified, all of which exhibited high expression in some or all of these tissues. Detailed information is provided in Table 1.

Table 1. Potential candidate genes highly expressed in tissues associated with the blood and immune system.

Gene Name	Blood and immune system				Protein expressed in the database of THE HUMAN PROTEIN ALTAS
	Bone marrow	Lymph node	Tonsil	Spleen	
CXCL12	High	Low	Low	Low	Bone marrow poietic cells showed strong nuclear positivity.
PTBP1	High	High	High	medium	Most normal tissues displayed strong nuclear positivity.
PKM2	Low	High	High	High	Cytoplasmic expression in most tissues, hepatocytes, neurons and most soft tissues were negative.
H2AFZ	High	High	medium	High	Ubiquitous nuclear expression.
NUDT1	medium	High	High	medium	Most normal tissues showed moderate to strong cytoplasmic staining.
ANGPT1	High	medium	medium	medium	Ubiquitous cytoplasmic expression.
PPAGR	low	not detected	High	low	Squamous epithelia, glandular cells in gastrointestinal tract, gall bladder, urinary bladder, placenta,epididymis showed moderate to strong nuclear positivity

 doi:10.20944/preprints202410.1444.v1

MME	medium	Low	medium	High	B-lymphocytes, myoepithelium, stromal cells and some glandular epithelia displayed strong cytoplasmic positivity.
RPS6KA2	medium	Low	High	medium	Most of the normal tissues displayed moderate nuclear and cytoplasmic positivity.
TTPAL	medium	High	High	High	Most normal tissues displayed moderate to strong cytoplasmic staining with a granular pattern.
BCL6	High	High	High	medium	Nuclear expression, mainly in lymphoid tissues.
CTNNB1	Low	not detected	High	not detected	Membranous expression was observed in most tissues.
STAT5A	medium	High	High	Low	Cytoplasmic and nuclear expression in a few tissues, most abundant in subsets of lymphoid cells.

Table 1. The primer sequences.

Primer information	Primer sequence
Gapdh qPCR Forward Primer	TGGCCTTCCGTGTTCCTAC
Gapdh qPCR Reverse Primer	GAGTTGCTGTTGAAGTCGCA
Alpl qPCR Forward Primer	GGCTGGAGATGGACAAATTCC
Alpl qPCR Reverse Primer	CCGAGTGGTAGTCACAATGCC
Bglap qPCR Forward Primer	CTGACCTCACAGATGCCAAGC
Bglap qPCR Reverse Primer	TGGTCTGATAGCTCGTCACAAG
H2afz qPCR Forward Primer	CCAAGACAAAGGCGGTTTCC
H2afz qPCR Reverse Primer	TTTCAGGTGTCGATGAATACGG
Bcl6 qPCR Forward Primer	CCGGCACGCTAGTGATGTT
Bcl6 qPCR Reverse Primer	GCACTGTCTTATGGGCTCTAAAC
Ttpal qPCR Forward Primer	GGCCTCACTCTCCGAAAATGA
Ttpal qPCR Reverse Primer	CAGGTATGGGTACTCCTTCCG
Ptbp1 qPCR Forward Primer	GCAGGCTGTAAACTCCGTCC
Ptbp1 qPCR Reverse Primer	GGGTCACTGGGTAGAAAAGGTT

Among the 13 candidates, four genes—PTBP1, H2AFZ, BCL6, and TTPAL (C20ORF121)—were found to have particularly high expression levels in most tissues related to the blood and immune system. Three of these genes were highly expressed across all four tissues, while one showed medium expression. These genes also demonstrated significant expression changes in the microarray data (Figure 3B).

The four genes, PTBP1, H2AFZ, TTPAL, and BCL6, serve as critical regulators of MSC osteogenic differentiation. Their potential roles in controlling this dynamic process make them promising targets for further investigation. We are currently conducting biological experiments to validate their molecular functions and further elucidate their involvement in MSC differentiation.

5. Isolation of bone mesenchymal stem cells and qRT–PCR identification of candidate genes during osteogenic induction

Bone marrow mesenchymal stem cells (BMSCs) are widely used in cell therapy and tissue engineering due to their self-renewal capacity and ability to differentiate into various mesoblastic cell types, including osteoblasts, chondrocytes, and adipocytes [30,31]. They are a type of multilineage progenitor cell that possesses self-renewal capacity and can differentiate into various types of mesoblastic cells, including osteoblasts, chondrocytes, adipocytes, etc. [32]. Given their significance, we isolated BMSCs to validate potential candidate genes identified through bioinformatics analysis.

We isolated BMSCs from bone marrow stem cells following standard protocols from the literature. To confirm their multilineage differentiation potential, we subjected the isolated cells to osteogenic, chondrogenic, and adipogenic induction, followed by Alizarin Red S (ARS), Alcian Blue,

 doi:10.20944/preprints202410.1444.v1

and Oil Red O staining. These results demonstrated that the isolated BMSCs retained their multilineage differentiation capacity (Figure 4A).

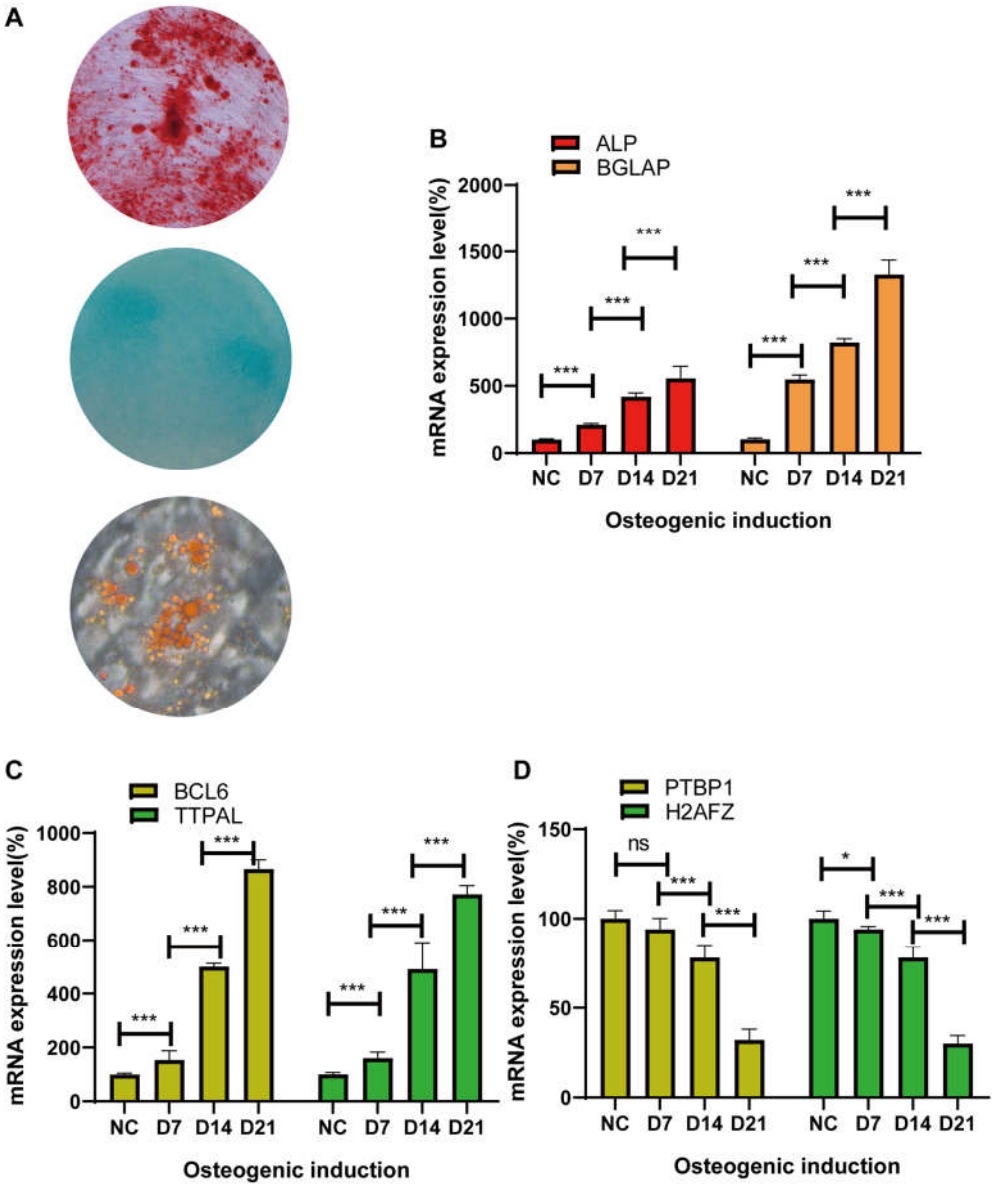

Figure 4. Elucidating the molecular m'sechanisms governing dynamic osteogenic induction in MSCs through the overexpression of four candidate genes using lentiviral packaging technology. (A) ARS, Alcian blue, and oil red O staining were used to detect the stem cell characteristics of BMSCs under osteogenic, chondrogenic, and adipogenic induction conditions; (B) qRT–PCR was used to detect osteogenic biomarkers at various induction time points; (C) qRT–PCR was used to detect BCL6 and TTPAL mRNA levels during the induction period in a time-dependent manner; and (D) qRT–PCR was used to detect PTBP1 and H2AFZ mRNA levels during the induction period in a time-dependent manner. All the experiments were conducted in triplicate, and a representative dataset was presented. All the data are presented as the means ± SDs. *$p < 0.05$; **$p < 0.01$ by Student's t test.

For osteogenic differentiation, we treated BMSCs with osteogenic medium and collected RNA at three time points: Day 7, Day 14, and Day 21. To assess osteogenesis, we measured the expression of key osteogenic biomarkers, ALP and BGLAP. The up-regulation of these biomarkers confirmed the success of the osteogenic differentiation experiment (Figure 4B).

Next, we evaluated the RNA expression of these four candidate genes—BCL6, TTPAL, PTBP1, and H2AFZ—which were identified through bioinformatics database mining. Using qRT-PCR, we assessed their RNA expression at various time points during osteogenic induction to validate our

 doi:10.20944/preprints202410.1444.v1

bioinformatic predictions. BCL6 and TTPAL showed sustained high expression throughout the induction period in a time-dependent manner (Figure 4C). Conversely, PTBP1 and H2AFZ exhibited continuous decreases in expression over time (Figure 4D).

These experimental results aligned with previous findings obtained from Gene Expression Omnibus (GEO) database analysis, confirming the accuracy of our bioinformatic predictions. This consistency provides a strong foundation for further research into the roles of these genes in MSC osteogenic differentiation.

6. **Identifying the molecular function of osteogenic regulators in MSCs via lentiviral overexpression of candidate genes**

To explore the molecular mechanisms that regulate osteogenic induction in MSCs, we performed lentiviral packaging technology to overexpress four potential regulatory genes: PTBP1, H2AFZ, BCL6, and TTPAL.

We first employed lentiviral packaging to overexpress the four candidate genes in 293T cells. The lentivirus produced from these cells was then used to infect bone marrow mesenchymal stem cells (BMSCs) using the 293T supernatant. After a 48-hour transduction period, RNA was extracted from the infected BMSCs to assess infection efficiency via qRT-PCR. The results confirmed successful infection, as shown in Figure 5A.

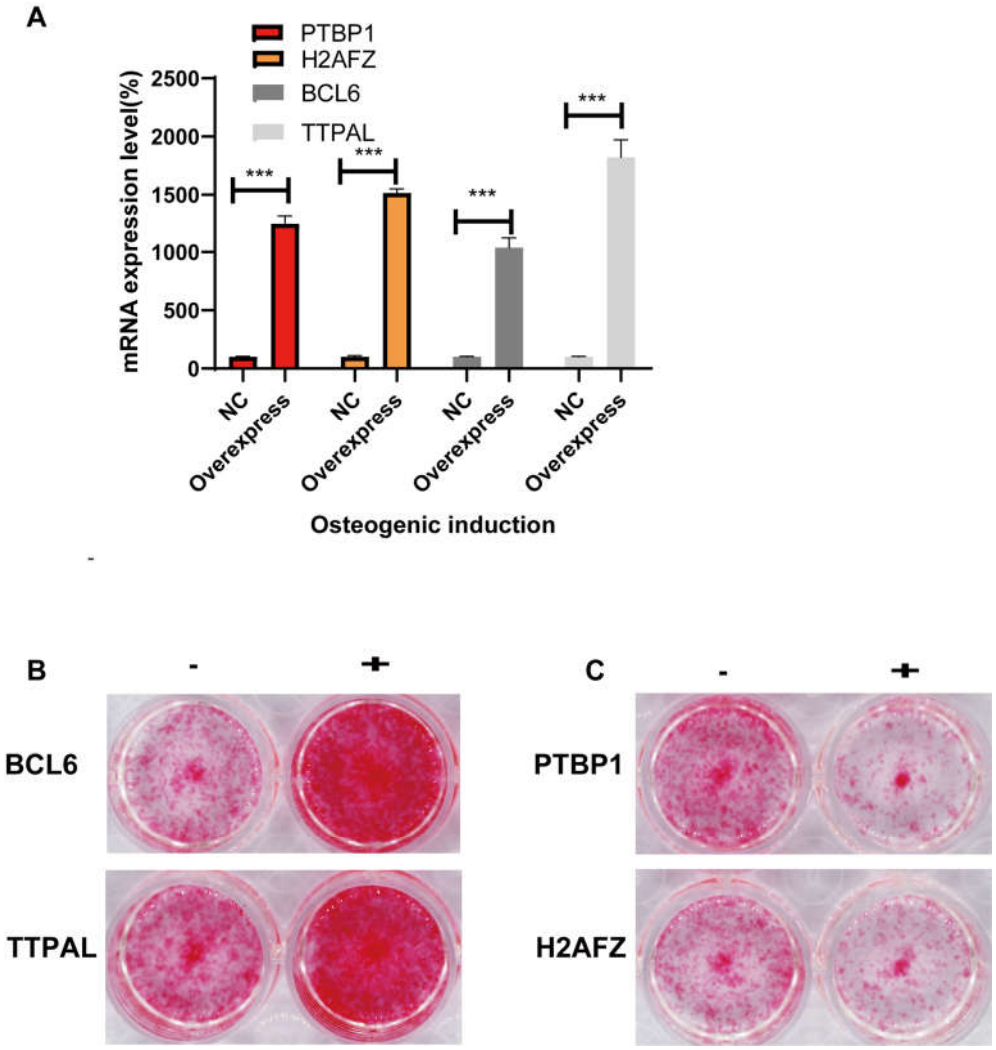

Figure 5. Molecular functions involved in the dynamic regulation of osteogenic induction through lentiviral-mediated overexpression of four candidate genes. (A) Overexpression efficacy measured by qRT–PCR; (B) Overexpression of BCL6 and TTPAL affects the osteogenic phenotype of BMSCs, as detected by an ALP assay; (C) Overexpression of PTBP1 and H2AFZ affects the osteogenic phenotype of BMSCs, as detected by an ALP assay. All the experiments were conducted in triplicate, and a

 doi:10.20944/preprints202410.1444.v1

representative dataset was presented. All the data are presented as the means ± SDs. *p < 0.05; **p < 0.01 by Student's t test.

To assess the impact of gene overexpression on osteogenesis, we performed experiments using lentiviruses containing each of the four genes to infect BMSCs. The osteogenic potential of the infected BMSCs was evaluated using an alkaline phosphatase (ALP) assay at Day 7 post-infection. A control group, infected with a vector virus, was used for comparison. BCL6 and TTPAL were shown to enhance osteogenic potential, as indicated by increased ALP activity (Figure 5B). In contrast, PTBP1 and H2AFZ appeared to inhibit osteogenesis, as demonstrated by reduced ALP activity (Figure 5C).

These findings suggest that BCL6 and TTPAL act as positive regulators of osteogenic differentiation in BMSCs, promoting osteogenic lineage commitment. Inversely, PTBP1 and H2AFZ function as negative regulators, inhibiting the osteogenic process. This dual role of these genes provides new insights into the molecular mechanisms underlying MSC osteogenic differentiation and may inform future therapeutic strategies for bone regeneration.

4. Discussion

With the advancement of omics, research on genome-wide dynamics, including transcription factors and epigenomic programming, during pre-osteoblast differentiation has made significant progress [33,34]. In this research article, we systematically investigated the dynamic regulation of MSC differentiation during osteogenesis by exploring key cellular factors. By integrating transcriptomic sequencing from different induction time points in a single-batch microarray dataset, as well as multiple-batch array sequencing, we identified 69 differentially expressed genes that exhibited continuous and significant changes during MSC osteogenic induction—49 of which were highly expressed, and 16 showed low expression.

To enhance the biological and clinical relevance of these candidate genes, we examined their expression levels in human tissues using the HUMAN PROTEIN ATLAS database [35]. High expression in blood and immune-related organs was used as a key criterion for further refining our selection. Through extensive big data analysis, we identified 13 genes with elevated expression in one or more blood and immune system tissues (Table 1).

Among these, four genes—PTBP1, H2AFZ, BCL6, and TTPAL—were selected for experimental validation due to their high expression in multiple blood and immune tissues. Our experimental results demonstrated dynamic changes in the expression of these genes during osteogenic induction, as shown in Figure 5A, which aligned with transcriptomic sequencing data. Moreover, the functional roles of these genes were confirmed through biological assays, as depicted in Figure 5B. These results validate our approach of combining transcriptome sequencing with big data mining to identify key targets that dynamically regulate biological functions.

This article represents the first to employ high-throughput transcriptomic sequencing to analyze and validate the key molecules that play a dynamic role that regulate MSC osteogenic differentiation in dynamics. This study holds great implications for understanding the molecular factors that influence MSC differentiation fate and could have significant clinical applications [36]. Specifically, the identification of PTBP1, H2AFZ, BCL6, and TTPAL as regulators of osteogenic differentiation presents novel therapeutic targets for conditions such as osteoporosis and bone fracture healing.

While our analysis of high-throughput transcriptomic data from the GEO database provided valuable insights into the biological processes underlying osteogenic differentiation [37], it is important to acknowledge the limitations of this approach. Single analyses, although informative, may not fully capture the complexity of these processes [38]. Future studies should adopt multi-omics approaches, integrating data from mRNAs, regulatory factors, proteins, and metabolites to construct comprehensive gene regulatory networks. This would help elucidate causal relationships between molecules and provide a deeper understanding of the underlying mechanisms [39].

 doi:10.20944/preprints202410.1444.v1

Despite this study focusing on high-throughput sequencing to identify key molecules in MSC osteogenic differentiation, further validation through both in vitro and in vivo experiments is necessary. This will help facilitate the translation of our findings into clinical applications [40].

Supplementary Materials: The following supporting information can be downloaded at the website of this paper posted on Preprints.org. Table S1: The primer sequences.

Author Contributions: Conceptualization, L.Y. and P.S.; methodology, L.L.; software, H.L.; validation, P.Y., L.T. and L.L.; formal analysis, P.Y.; investigation, H.L.; resources, L.T.; data curation, L.T.; writing—original draft preparation, X.X.; writing—review and editing, X.X.; visualization, X.X.; supervision, P.S.; project administration, L.L.; funding acquisition, L.Y. and L.T. All authors have read and agreed to the published version of the manuscript.

Funding: This research was funded by NATURAL SCIENCE FOUNDATION OF JIANGSU PROVINCE, grant number BK20221288 to Tao Liu, CHINA POSTDOCTORAL SCIENCE FOUNDATION, grant number 2020M681232 to Yuwei Liu and NATIONAL NATURAL SCIENCE FOUNDATION OF CHINA, grant number 82101630 to Yuwei Liu.

Institutional Review Board Statement: All animal studies were performed in accordance with protocols approved by the Institutional Animal Care and Use Committee of East China Normal University (ECNU). All mice had unrestricted access to food, water, and activity and were housed under a 12 h dark-light cycle with a constant temperature (20 ~ 26 °C) and humidity maintenance (40 – 60 %). All animal experiments were conducted under license at the Institutional Animal Care and Use Committee at East China Normal University (project license m20210216). For euthanasia, mice were exposed to carbon dioxide with a Smartbox setup with a flow meter to calculate to deliver the appropriate flow, followed by cervical dislocation.

Informed Consent Statement: Not applicable.

Data Availability Statement: Data supporting our study are openly available in public repositories GSE37558 and GSE28205.

Acknowledgments: No.

Conflicts of Interest: The authors declare no conflicts of interest.

References

1. Yu H, Huang Y, Yang L. Research progress in the use of mesenchymal stem cells and their derived exosomes in the treatment of osteoarthritis. Ageing Res Rev. 2022;80:101684.
2. Zhang H, Xu R, Li B, Xin Z, Ling Z, Zhu W, et al. LncRNA NEAT1 controls the lineage fates of BMSCs during skeletal aging by impairing mitochondrial function and pluripotency maintenance. Cell Death Differ. 2022;29(2):351-65.
3. Han Y, Yang J, Fang J, Zhou Y, Candi E, Wang J, et al. The secretion profile of mesenchymal stem cells and potential applications in treating human diseases. Signal Transduct Target Ther. 2022;7(1):92.
4. Wang Y, Fang J, Liu B, Shao C, Shi Y. Reciprocal regulation of mesenchymal stem cells and immune responses. Cell Stem Cell. 2022;29(11):1515-30.
5. Jiang Z, Li N, Shao Q, Zhu D, Feng Y, Wang Y, et al. Light-controlled scaffold- and serum-free hard palatal-derived mesenchymal stem cell aggregates for bone regeneration. Bioeng Transl Med. 2023;8(1):e10334.
6. Li P, Gong Z, Shultz LD, Ren G. Mesenchymal stem cells: From regeneration to cancer. Pharmacol Ther. 2019;200:42-54.
7. Hoang DM, Pham PT, Bach TQ, Ngo ATL, Nguyen QT, Phan TTK, et al. Stem cell-based therapy for human diseases. Signal Transduct Target Ther. 2022;7(1):272.
8. Zhang L, Ma XJ, Fei YY, Han HT, Xu J, Cheng L, et al. Stem cell therapy in liver regeneration: Focus on mesenchymal stem cells and induced pluripotent stem cells. Pharmacol Ther. 2022;232:108004.
9. Song N, Scholtemeijer M, Shah K. Mesenchymal Stem Cell Immunomodulation: Mechanisms and Therapeutic Potential. Trends Pharmacol Sci. 2020;41(9):653-64.
10. Kim P, Park J, Lee DJ, Mizuno S, Shinohara M, Hong CP, et al. Mast4 determines the cell fate of MSCs for bone and cartilage development. Nat Commun. 2022;13(1):3960.
11. Deng P, Yuan Q, Cheng Y, Li J, Liu Z, Liu Y, et al. Loss of KDM4B exacerbates bone-fat imbalance and mesenchymal stem cell exhaustion in skeletal aging. Cell Stem Cell. 2021;28(6):1057-73.e7.
12. Liu F, Yuan Y, Bai L, Yuan L, Li L, Liu J, et al. LRRc17 controls BMSC senescence via mitophagy and inhibits the therapeutic effect of BMSCs on ovariectomy-induced bone loss. Redox Biol. 2021;43:101963.
13. Li CJ, Xiao Y, Yang M, Su T, Sun X, Guo Q, et al. Long noncoding RNA Bmncr regulates mesenchymal stem cell fate during skeletal aging. J Clin Invest. 2018;128(12):5251-66.

14. Li W, Feng W, Su X, Luo D, Li Z, Zhou Y, et al. SIRT6 protects vascular smooth muscle cells from osteogenic transdifferentiation via Runx2 in chronic kidney disease. J Clin Invest. 2022;132(1).
15. Xing W, Godwin C, Pourteymoor S, Mohan S. Conditional disruption of the osterix gene in chondrocytes during early postnatal growth impairs secondary ossification in the mouse tibial epiphysis. Bone Res. 2019;7:24.
16. Yoshida G, Kawabata T, Takamatsu H, Saita S, Nakamura S, Nishikawa K, et al. Degradation of the NOTCH intracellular domain by elevated autophagy in osteoblasts promotes osteoblast differentiation and alleviates osteoporosis. Autophagy. 2022;18(10):2323-32.
17. Liu ZZ, Hong CG, Hu WB, Chen ML, Duan R, Li HM, et al. Autophagy receptor OPTN (optineurin) regulates mesenchymal stem cell fate and bone-fat balance during aging by clearing FABP3. Autophagy. 2021;17(10):2766-82.
18. Zhang Y, Lin D, Zheng Y, Chen Y, Yu M, Cui D, et al. MiR-9-1 controls osteoblastic regulation of lymphopoiesis. Leukemia. 2023.
19. Lee KS, Lee J, Kim HK, Yeom SH, Woo CH, Jung YJ, et al. Extracellular vesicles from adipose tissue-derived stem cells alleviate osteoporosis through osteoprotegerin and miR-21-5p. J Extracell Vesicles. 2021;10(12):e12152.
20. Lim J, Heo J, Ju H, Shin JW, Kim Y, Lee S, et al. Glutathione dynamics determine the therapeutic efficacy of mesenchymal stem cells for graft-versus-host disease via CREB1-NRF2 pathway. Sci Adv. 2020;6(16):eaba1334.
21. Soliman H, Theret M, Scott W, Hill L, Underhill TM, Hinz B, et al. Multipotent stem cells: One name, multiple identities. Cell Stem Cell. 2021;28(10):1690-707.
22. Zong C, Meng Y, Ye F, Yang X, Li R, Jiang J, et al. AIF1 + CSF1R + MSCs, induced by TNF-α, act to generate an inflammatory microenvironment and promote hepatocarcinogenesis. Hepatology. 2023;78(2):434-51.
23. Tsai JN, Lee H, David NL, Eastell R, Leder BZ. Combination denosumab and high dose teriparatide for postmenopausal osteoporosis (DATA-HD): a randomised, controlled phase 4 trial. Lancet Diabetes Endocrinol. 2019;7(10):767-75.
24. Wang Y, Deng P, Liu Y, Wu Y, Chen Y, Guo Y, et al. Alpha-ketoglutarate ameliorates age-related osteoporosis via regulating histone methylations. Nat Commun. 2020;11(1):5596.
25. Cai W, Zhang J, Yu Y, Ni Y, Wei Y, Cheng Y, et al. Mitochondrial Transfer Regulates Cell Fate Through Metabolic Remodeling in Osteoporosis. Adv Sci (Weinh). 2023;10(4):e2204871.
26. Gong Y, Li Z, Zou S, Deng D, Lai P, Hu H, et al. Vangl2 limits chaperone-mediated autophagy to balance osteogenic differentiation in mesenchymal stem cells. Dev Cell. 2021;56(14):2103-20.e9.
27. Tsukasaki M, Takayanagi H. Osteoimmunology: evolving concepts in bone-immune interactions in health and disease. Nat Rev Immunol. 2019;19(10):626-42.
28. Hochmann S, Ou K, Poupardin R, Mittermeir M, Textor M, Ali S, et al. The enhancer landscape predetermines the skeletal regeneration capacity of stromal cells. Sci Transl Med. 2023;15(688):eabm7477.
29. Mo C, Guo J, Qin J, Zhang X, Sun Y, Wei H, et al. Single-cell transcriptomics of LepR-positive skeletal cells reveals heterogeneous stress-dependent stem and progenitor pools. Embo j. 2022;41(4):e108415.
30. Guo Y, Jia X, Cui Y, Song Y, Wang S, Geng Y, et al. Sirt3-mediated mitophagy regulates AGEs-induced BMSCs senescence and senile osteoporosis. Redox Biol. 2021;41:101915.
31. Jiao D, Zheng A, Liu Y, Zhang X, Wang X, Wu J, et al. Bidirectional differentiation of BMSCs induced by a biomimetic procallus based on a gelatin-reduced graphene oxide reinforced hydrogel for rapid bone regeneration. Bioact Mater. 2021;6(7):2011-28.
32. Zhang P, Dong J, Fan X, Yong J, Yang M, Liu Y, et al. Characterization of mesenchymal stem cells in human fetal bone marrow by single-cell transcriptomic and functional analysis. Signal Transduct Target Ther. 2023;8(1):126.
33. Cui J, Shibata Y, Zhu T, Zhou J, Zhang J. Osteocytes in bone aging: Advances, challenges, and future perspectives. Ageing Res Rev. 2022;77:101608.
34. Delgado-Calle J, Bellido T. The osteocyte as a signaling cell. Physiol Rev. 2022;102(1):379-410.
35. Sjöstedt E, Zhong W, Fagerberg L, Karlsson M, Mitsios N, Adori C, et al. An atlas of the protein-coding genes in the human, pig, and mouse brain. Science. 2020;367(6482).
36. Cherubini A, Barilani M, Rossi RL, Jalal MMK, Rusconi F, Buono G, et al. FOXP1 circular RNA sustains mesenchymal stem cell identity via microRNA inhibition. Nucleic Acids Res. 2019;47(10):5325-40.
37. Yang M, Miao YR, Xie GY, Luo M, Hu H, Kwok HF, et al. ICBatlas: A Comprehensive Resource for Depicting Immune Checkpoint Blockade Therapy Characteristics from Transcriptome Profiles. Cancer Immunol Res. 2022;10(11):1398-406.
38. Ma Q, Xu D. Deep learning shapes single-cell data analysis. Nat Rev Mol Cell Biol. 2022;23(5):303-4.
39. Gao Y, Chi Y, Chen Y, Wang W, Li H, Zheng W, et al. Multi-omics analysis of human mesenchymal stem cells shows cell aging that alters immunomodulatory activity through the downregulation of PD-L1. Nat Commun. 2023;14(1):4373.

 doi:10.20944/preprints202410.1444.v1

40. Deng C, Dong K, Liu Y, Chen K, Min C, Cao Z, et al. Hypoxic mesenchymal stem cell-derived exosomes promote the survival of skin flaps after ischaemia-reperfusion injury via mTOR/ULK1/FUNDC1 pathways. J Nanobiotechnology. 2023;21(1):340.